

New Hybrid Nanomaterial Derived from Immobilization of 4-Formyl Benzo-9-Crown-3 Ether onto the Mesopores of MCM-41

M. Masteri-Farahani^{*1}, R. Rahimpour²

¹Faculty of Chemistry, Kharazmi University, Tehran, Islamic Republic of Iran

²Faculty of Chemistry, Islamic Azad University, Ardebil branch, Ardebil, Islamic Republic of Iran

Received: 6 September 2015 / Revised: 4 February 2016 / Accepted: 30 April 2016

Abstract

In this work, we report a new hybrid nanomaterial based on the immobilization of 4-formyl benzo-9-crown-3 ether (FB9C3) onto the mesopores of MCM-41. First, the mesoporous molecular sieve MCM-41 was covalently grafted with 3-aminopropyl triethoxysilane to give aminopropyl modified MCM-41 (AmpMCM-41). Reaction of this material with FB9C3 afforded the B9C3-AmpMCM-41 hybrid nanomaterial. The prepared B9C3-AmpMCM-41 was characterized with different physicochemical methods such as Fourier transform infrared spectroscopy, X-ray diffraction (XRD), scanning and transmission electron microscopy, thermogravimetric analysis (TGA-DTA), and BET nitrogen adsorption-desorption analysis. The XRD analysis revealed that textural properties of the support were preserved during the immobilization process. However, nitrogen adsorption-desorption analysis showed sequential reduction in surface area, pore volume, and pore size during the grafting experiments. Elemental analysis showed the presence of 0.11 mmol FB9C3 per gram of the hybrid nanomaterial.

Keywords: Mesoporous; MCM-41; Hybrid nanomaterial; Benzo-9-crown-3 ether; Immobilization.

Introduction

The field of organic-inorganic hybrid materials is expanding because of their important role in the development of advanced functional materials [1-8]. In this regard, design and construction of organic-inorganic hybrid nanomaterials with tunable physical properties have attracted extensive research interest in materials chemistry. Inorganic-organic hybrid materials can be grossly divided into two major classes: Class I in which only weak bonds exist and class II in which the

building blocks are connected by covalent bonds.

Hybrid materials of MCM-41 take advantage of the properties of the MCM-41 support, as well as of the immobilized surface groups [7-9]. The advantages of MCM-41 such as its high surface area and porous structure support it as an ideal building block in hybrid materials. On the other hand, hybridization results in materials with high specific surface areas that allow the use of less material, reducing cost and toxicity.

In recent years, various methods for functionalizing the surfaces of MCM-41 with different groups have

* Corresponding author: Tel: +982634551023; Fax: +982634551023; Email: mfarahany@yahoo.com

been investigated as the surface modification permits tailoring of the surface properties for numerous potential applications including catalysis [8-15], enzyme immobilization [16], environmental pollution management [17-18], and electrochemistry [19-20].

Macrocycles of the $(-\text{CH}_2-\text{CH}_2\text{O}-)_n$ type in which $n \geq 4$ are generally referred to as crown ethers [21]. The essential repeating unit of simple crown ethers is ethyleneoxy $-\text{CH}_2-\text{CH}_2\text{O}-$ unit. The nine-membered ring 1,4,7-trioxonane (9-crown-3) is also named as a crown and can certainly interact with cations. Complexation by 9-crown-3 (often two molecules per cation) is known but less common. The most important property of crown ethers is their ability to form stable complexes with metal ions, organic cations, and neutral polar molecules. This forms the basis for the use of crown ethers as selective ligands coordinated to metal cations, including their use for extraction [22-23], in ion selective electrodes [24], photosensitive systems [25], etc.

Our current interest in the preparation of hybrid materials with potential applications in catalysis of organic reactions [10-13,26-28] and selective adsorbents for metal cations [29-30] led us to investigate the preparation and characterization of B9C3-AmpMCM-41 hybrid nanomaterial which belongs to the type II of organic-inorganic hybrid materials. The prepared hybrid nanomaterial is predicted to have interesting properties as selective adsorbent for metal cations and also application in ion selective electrodes.

Materials and Methods

All chemicals were purchased from Merck chemical company and used without further purification. The 4-formyl benzo-9-crown-3 ether was prepared and characterized according to the literature method [31].

Fourier transform infrared spectra were recorded using Perkin-Elmer Spectrum RXI FT-IR spectrometer, using pellets of the materials diluted with KBr. Powder X-ray diffraction data were collected with a SIEFERT XRD 3003 PTS diffractometer using $\text{Cu K}\alpha$ radiation. Carbon and nitrogen content of the samples was analyzed on Thermo Finnigan (Flash 1112 Series EA) CHN Analyzer. Thermogravimetric analysis (TGA) of the samples was performed using a Perkin Elmer Diamond Thermogravimeter. Dried samples was placed in the TGA furnace and heated at a rate of $10^\circ\text{C min}^{-1}$ from room temperature to 700°C in static air. *Nitrogen sorption studies were performed at liquid nitrogen temperature (77 K) using Quanta chrome Nova 2200, Version 7.11 Analyzer. Before the adsorption experiments the samples were outgassed under nitrogen*

gas at 120°C . All calculations were performed using the program of Quantachrome Nova 2200e surface area analyzer. The morphology of the product was observed by using ZEISS-DSM 960A scanning electron microscope with attached camera operating at 30 kV.

Preparation of MCM-41 and aminopropyl modified MCM-41 (AmpMCM-41)

Mesoporous molecular sieve MCM-41 was prepared according to the literature method [32]. Modification of the prepared MCM-41 was carried out as follows: MCM-41 (2 g) was suspended in dry toluene (60 ml) and aminopropyl triethoxysilane (1 g) was then added to the resulted mixture. The resulting mixture was refluxed for 24 hours under dry nitrogen atmosphere. After filtration and washing with dichloromethane and ethanol, the solid was dried. The resulting material was then soxhlet extracted with dichloromethane to remove the residue of silylating reagent and then vacuum dried at 120°C .

Preparation of B9C3-AmpMCM-41 hybrid nanomaterial

Immobilization of the 4-formyl benzo-9-crown-3 ether for the preparation of hybrid nanomaterial was achieved according to the standard method used for the synthesis of Schiff bases. A mixture of vacuum dried AmpMCM-41 (1.5 g) in 25 ml absolute ethanol and 3 mmol of 4-formyl benzo-9-crown-3 ether was refluxed for 24 hours under dry nitrogen atmosphere to afford MCM-41 supported benzo-9-crown-3 ether, B9C3-AmpMCM-41. The solid was filtered, and then soxhlet extracted with ethanol to remove the unreacted 4-formyl benzo-9-crown-3 ether and dried under vacuum at 120°C overnight.

Results and Discussion

Preparation of the B9C3-AmpMCM-41 hybrid nanomaterial

The sequence of processes for the preparation of B9C3-AmpMCM-41 hybrid material is represented in Figure 1. In the first step, condensation of the surface hydroxyl groups of MCM-41 with the ethoxy groups of aminopropyl triethoxysilane forms stable covalent Si-O-Si linkage, leading to the attachment of aminopropyl groups on the surface of MCM-41. In this grafting reaction mainly two ethoxy groups of the silylating agent were replaced by silanol groups of the surface [33]. The condensation reaction modifies both external and inner channel silanol groups. However, since the high surface area in MCM-41 can be attributed to the pore system, functionalization occurs predominantly on

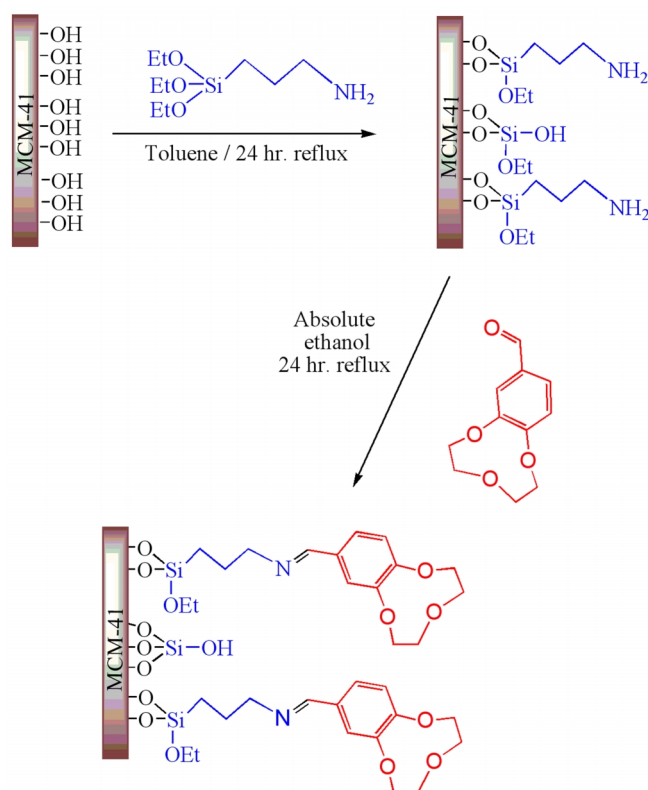


Figure 1. The sequence of processes in the preparation of B9C3-AmpMCM-41 hybrid nanomaterial

the internal surface. In the next step, Schiff base condensation of the amine groups of resulting AmpMCM-41 with carbonyl groups of 4-formyl benzo-9-crown-3 ether gives rise to the preparation of B9C3-AmpMCM-41 hybrid nanomaterial. In this reaction, the amine group of AmpMCM-41 and carbonyl group of 4-formyl benzo-9-crown-3 ether are condensed to afford

imine bond through which the crown ether is attached onto the inner surface of MCM-41.

Characterization of the B9C3-AmpMCM-41 hybrid nanomaterial

In order to confirm the modification of MCM-41 surface, the FT-IR spectra of the MCM-41, B9C3-

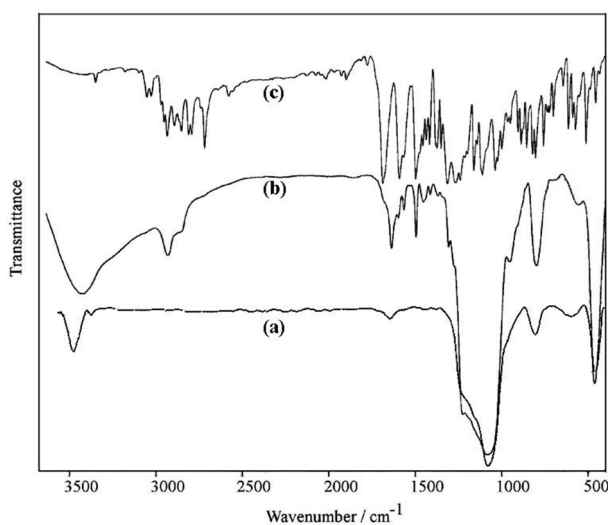


Figure 2. FT-IR spectra of (a) MCM-41, (b) B9C3-AmpMCM-41, and (c) B9C3

Table 1. Texture parameters of samples obtained from XRD

Sample	$2\theta / ^\circ$	XRD d_{100} value (\AA)	Lattice parameter ^a (\AA)
MCM-41	2.71	32.6	37.6
AmpMCM-41	2.65	33.3	38.4
B9C3-AmpMCM-41	2.56	34.6	40

^a Determined by equation: $a_0 = d_{100} (2/\sqrt{3})$

AmpMCM-41, and FB9C3 were obtained and have been shown in Figure 2. The broad peak at about $1000\text{--}1200\text{ cm}^{-1}$ in the FT-IR spectra of MCM-41 (Figure 2a) and B9C3-AmpMCM-41 (Figure 2b) are assigned to Si-O-Si asymmetric stretching vibrations. The FT-IR spectrum of B9C3-AmpMCM-41 showed the characteristic band of the propyl groups ($\nu_{\text{C-H}}$) at 2964 cm^{-1} which were not present in the FT-IR spectrum of MCM-41. On the other hand, in the FT-IR spectrum of B9C3-AmpMCM-41 the observation of the band at 1626 cm^{-1} was attributed to the stretching vibration of C=N bond and some weak bands observed at $1400\text{--}1500\text{ cm}^{-1}$ was assigned to stretching vibrations of aromatic rings in 4-formyl benzo-9-crown-3 ether. The absence of these bands in the parent MCM-41 proved the successful grafting of the 4-formyl benzo-9-crown-3 ether to the surface of MCM-41.

On the other hand, the amount of functionalization with aminopropyl groups was found to be 0.1 mmol.g^{-1} on the basis of nitrogen content measurement.

Textural properties of the materials were investigated with X-ray diffraction and BET adsorption-desorption analyses. X-ray diffraction patterns of MCM-41, AmpMCM-41, and B9C3-AmpMCM-41 hybrid material are shown in Figure 3 and corresponding

texture parameters are given in Table 1. In the X-ray diffraction pattern of unmodified MCM-41 (Figure 3a), the strong reflection at $2\theta = 2.71$ belongs to $\langle 100 \rangle$ reflection and three weaker reflections at higher angles arise from $\langle 110 \rangle$, $\langle 200 \rangle$ and $\langle 210 \rangle$ reflections of a hexagonal unit cell. The hexagonal unit cell parameter a_0 (or lattice parameter), a measure of d-spacing present between the hexagonal layers, is calculated as $d_{100} (2/\sqrt{3})$. The XRD patterns of the AmpMCM-41 and B9C3-AmpMCM-41 hybrid nanomaterial (Figures 3b-c) show only the $\langle 100 \rangle$ reflection with lower intensity and the other reflections have been disappeared partly due to a decrease in the mesoscopic order of the materials and mainly due to the contrast matching between the silicate framework and organic moieties located inside the MCM-41 channels [34]. Also the position of this reflection shifted to lower angles (or higher d-values) that indicates the expansion of unit cell parameter due to the incorporation of organic groups within MCM-41. Incorporation of FB9C3 moiety resulted in shifting the $\langle 100 \rangle$ reflection to lower angles (or higher d-values) with respect to that of MCM-41 and AmpMCM-41. As a result, this indicates further unit cell expansion in comparison with AmpMCM-41.

Mesoporous texture of the MCM-41, AmpMCM-41,

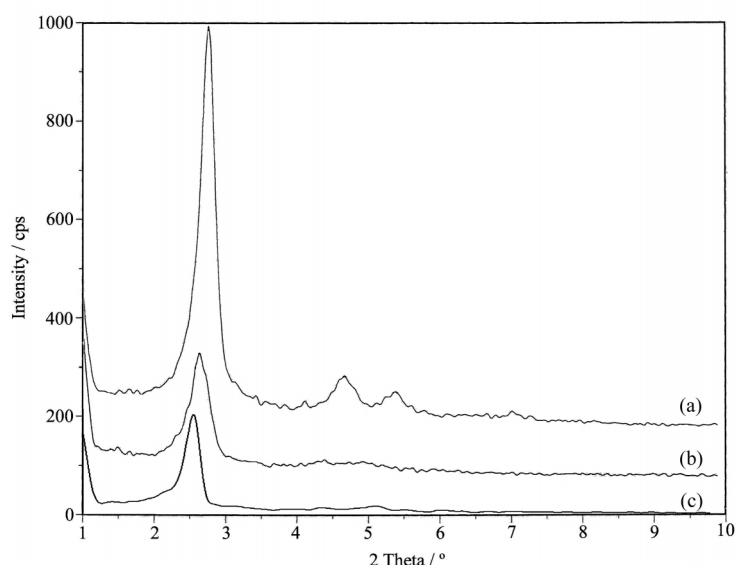


Figure 3. XRD patterns of (a) MCM-41, (b) AmpMCM-41, and (c) B9C3-AmpMCM-41 hybrid nanomaterial

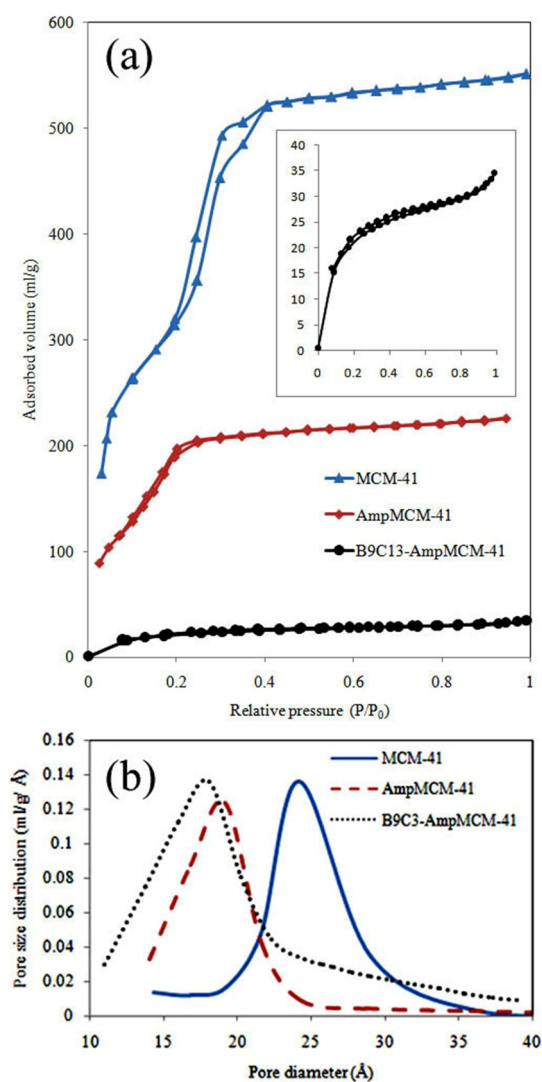


Figure 4. (a) Nitrogen adsorption-desorption isotherms and (b) BJH pore size distributions of prepared materials

and B9C3-AmpMCM-41 hybrid nanomaterial was further controlled by nitrogen sorption analyses. The adsorption-desorption isotherms of N_2 at 77 K for MCM-41, AmpMCM-41, and B9C3-AmpMCM-41 hybrid nanomaterial (Figure 4a) show hysteresis loops which indicate the presence of mesoporosity in these materials and exhibits type IV isotherm according to the

Brunauer-Deming-Deming-Teller (BDDT) classification [35]. In the adsorption isotherm of AmpMCM-41 and B9C3-AmpMCM-41, the inflection point shifts to lower relative pressures and the volume of nitrogen adsorbed decreases upon functionalization. As expected, this indicates the presence of aminopropyl and FB9C3 groups tethered to the pore walls of the mesopores. On the basis of the nitrogen sorption studies of the B9C3-AmpMCM-41 hybrid nanomaterial we can reveal the location of the 4-formyl benzo-9-crown-3 ether on the surface of MCM-41. As can be seen in Figure 4a, there is considerable difference in the adsorption of N_2 in the B9C3-AmpMCM-41 hybrid nanomaterial with respect to the original MCM-41 support. In the case of B9C3-AmpMCM-41 the amount of nitrogen uptake decreased dramatically which means that the 4-formyl benzo-9-crown-3 ether has been introduced to the internal surface of MCM-41. Pore size distributions were obtained from the desorption branch of the isotherms using the Barrett, Joyner and Halenda (BJH) method and are shown in Figure 4b. All materials show maxima indicating the presence of mesopores. The texture parameters of the materials derived from nitrogen sorption analysis are collected in Table 2. Determination of total surface area is commonly based on the BET theory of multilayer adsorption with the relative pressure (p/p_0) in range of 0.05–0.30. In comparison with MCM-41, the B9C3-AmpMCM-41 hybrid nanomaterial shows a decrease of specific surface area due to incorporation of 4-formyl benzo-9-crown-3 ether onto the mesopores of MCM-41. The total pore volume was directly calculated from the volume of nitrogen held at the highest relative pressure ($p/p_0 = 0.98$), using 0.8081 g.cm^{-3} for the density of N_2 in its normal liquid state. As can be seen, the total pore volume was decreased with immobilization of 4-formyl benzo-9-crown-3 ether onto the mesopores of MCM-41. These results reveal that incorporation of FB9C3 lead to specific surface area reduction of prepared materials. This trend is almost inverted with respect to that observed in unit cell parameters of the materials. It can be deduced that decrease of unit cell parameter is equal to increase of specific surface area of the materials and vice versa.

The thermal behavior of the B9C3-AmpMCM-41

Table 2. Texture parameters of samples taken from nitrogen sorption studies

Sample	S_{BET} ($\text{m}^2 \cdot \text{g}^{-1}$)	V_{T}^{a} ($\text{mL} \cdot \text{g}^{-1}$)	Pore diameter ^b (nm)
MCM-41	1211	0.85	2.8
AmpMCM-41	753	0.35	1.9
B9C3-AmpMCM-41	76	0.04	1.7

^a Total pore volume at $p/p_0 = 0.98$.

^b Calculated based on the desorption isotherm branch using the BJH method.

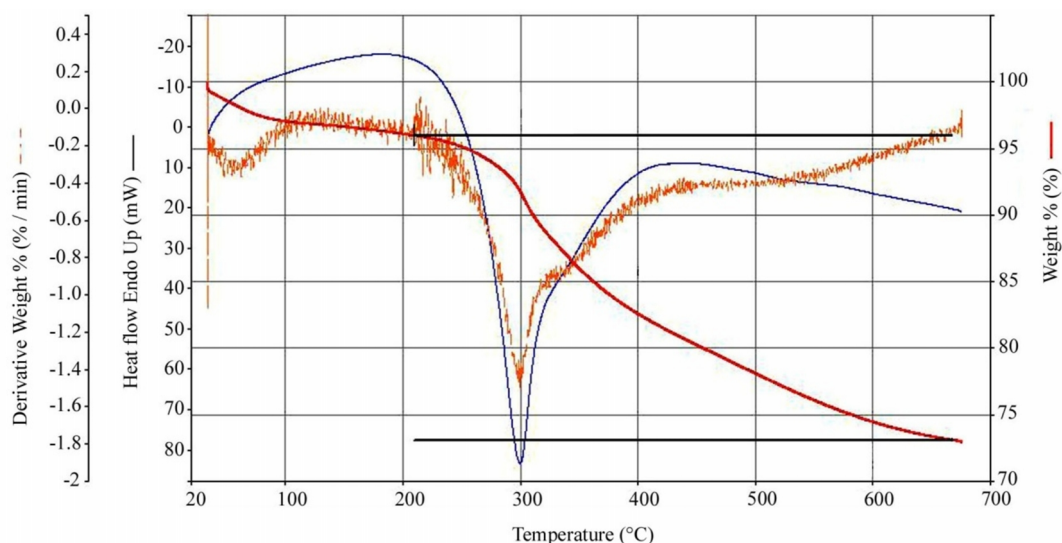


Figure 5. TGA-DTA curves of prepared B9C3-AmpMCM-41 hybrid nanomaterial

was investigated by TGA-DTA analysis. Figure 5 shows the TGA and DTA curves for the prepared B9C3-AmpMCM-41. The TGA curve indicates two stages of mass reduction as a function of temperature. The first stage, about 50-200°C, was ascribed to the loss of adsorbed water. Due to the hydrophobic nature of the prepared hybrid material the amount of adsorbed water was only about 4 wt%. The corresponding DTA curve in this region is endothermic because the removal of adsorbed water is endothermic. The second stage about 200-500°C was assigned to the combustion of organic compounds, which is in good agreement with exothermic DTA peak in this region.

A typical scanning electron micrograph of the prepared B9C3-AmpMCM-41 has been shown in Figure 6a. The SEM image indicates that the obtained nanoparticles are composed of nearly uniform ellipsoids with some agglomerations.

On the other hand, the morphology and microstructure of the prepared material were investigated by TEM analysis (Figure 6b). From Figure 6b, highly ordered mesoporous structure and a narrow pore distribution can be observed. This indicates that the mesoporous structure of MCM-41 is maintained after the immobilization of 4-formyl benzo-9-crown-3 ether.

In summary, reaction of the 4-formyl benzo-9-crown-3 ether with aminopropyl silyl modified MCM-41 afforded B9C3-AmpMCM-41 hybrid nanomaterial in which the crown ether moiety was attached through propyl chain spacer. Characterization of the prepared nanomaterial was performed with different physicochemical methods. The prepared nanomaterial

predicts to have interesting properties as selective adsorbent for metal cations and also application in ion

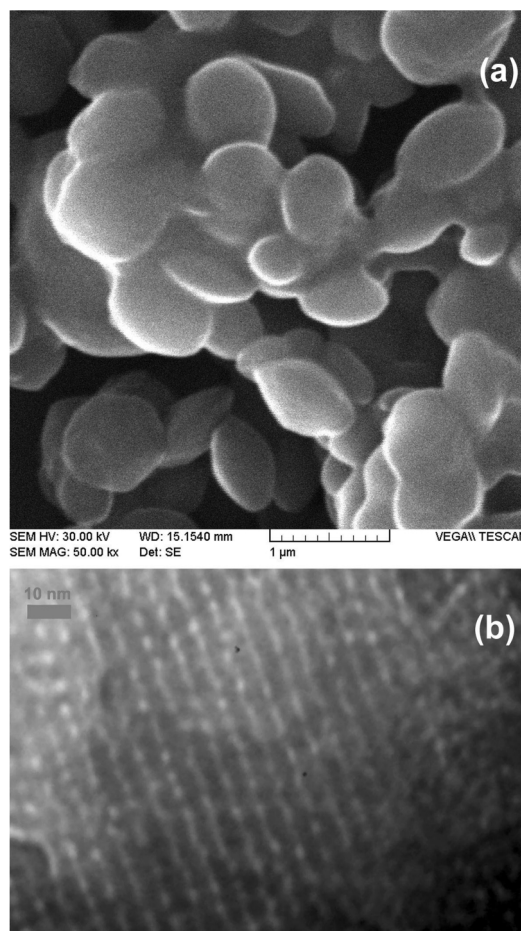


Figure 6. (a) SEM and (b) TEM images of the B9C3-AmpMCM-41 hybrid nanomaterial

selective electrodes.

References

- Sanchez C., Julian B., Belleville P., Popall M., Applications of hybrid organic-inorganic nanocomposites, *J. Mater. Chem.* **15**: 3559-3592 (2005).
- Kickelbick G., *Hybrid Materials. Synthesis, Characterization, and Applications*, ed. G. Kickelbick, Wiley-VCH, Weinheim, (2007).
- Eder D., Carbon Nanotube-Inorganic Hybrids, *Chem. Rev.* **110**: 1348-1385 (2010).
- Moreau J.J.E., Man M.W.C., The design of selective catalysts from hybrid silica-based materials, *Coord. Chem. Rev.* **178-180**: 1073-1084 (1998).
- Cerveau G., Corriu R.J.P., Framery E., Nanostructured Organic Inorganic Hybrid Materials: Kinetic Control of the Texture, *Chem. Mater.* **13**: 3373-3388 (2001).
- Ashby M.F., Brechet Y.J.M., Designing hybrid materials, *Acta Mater.* **51**: 5801-5821 (2003).
- Hoffmann F., Cornelius M., Morell J., Froba M., Silica-Based Mesoporous Organic-Inorganic Hybrid Materials, *Angew. Chem. Int. Ed.* **45**: 3216-3251 (2006).
- Valkenberg M.H., Holderich W.F., Preparation and use of hybrid organic-inorganic catalysts, *Catal. Rev.* **44**: 321-374 (2002).
- Wight A.P., Davis M.E., Design and Preparation of Organic-Inorganic Hybrid Catalysts, *Chem. Rev.* **102**: 3589-3614 (2002).
- Masteri-Farahani M., Farzaneh F., Ghandi M., Synthesis and Characterization of cis-MoO₂ (salpr) Complex grafted MCM-41 as Selective Catalyst for Epoxidation of Olefins, *J. Mol. Catal. A: Chem.* **243**: 170-175 (2006).
- Masteri-Farahani M., Farzaneh F., Ghandi M., Synthesis of tetradentate N₄ Schiff base dioxomolybdenum (VI) complex within MCM-41 as selective catalyst for epoxidation of olefins, *Catal. Commun.* **8**: 6-10 (2007).
- Masteri-Farahani M., Farzaneh F., Ghandi M., Synthesis and characterization of molybdenum complexes with bidentate Schiff base ligands within nanoreactors of MCM-41 as epoxidation catalysts, *J. Mol. Catal. A: Chem.* **248**: 53-60 (2006).
- Masteri-Farahani M., *Investigation of catalytic activities of new heterogeneous molybdenum catalysts in epoxidation of olefins*, *J. Mol. Catal. A: Chem.* **316**: 45-51 (2010).
- Jia M., Seifert A., Thiel W.R., Mesoporous MCM-41 Materials Modified with Oxodiperoxo Molybdenum Complexes: Efficient Catalysts for the Epoxidation of Cyclooctene, *Chem. Mater.* **15**: 2174-2180 (2003).
- Bruno S.M., Fernandes J.A., Martins L.S., Goncalves I.S., Pillinger M., Ribeiro-Claro P., Rocha J., Valente A.A., Dioxomolybdenum (VI) modified mesoporous materials for the catalytic epoxidation of olefins, *Catal. Today* **114**: 263-271 (2006).
- Lee C.H., Lin T.S., Mou C.Y., Mesoporous materials for encapsulating enzymes, *NanoToday* **4**: 165-179 (2009).
- Sayari A., Hamoudi S., Yang Y., Applications of Pore-Expanded Mesoporous Silica.1. Removal of Heavy Metal Cations and Organic Pollutants from Wastewater, *Chem. Mater.* **17**: 212-216 (2005).
- Lee C.K., Liu S.S., Juang L.C., Wang C.C., Lin K.S., Lyu M.D., Application of MCM-41 for dyes removal from wastewater, *J. Hazard. Mater.* **147**: 997-1005 (2007).
- Walcarius A., Impact of mesoporous silica-based materials on electrochemistry and feedback from electrochemical science to the characterization of these ordered materials, *C.R. Chimie* **8**: 693-712 (2005).
- Walcarius A., Analytical Applications of Silica-Modified Electrodes-A Comprehensive Review, *Electroanalysis* **10**: 1217-1235 (1998).
- Pedersen C.J., Cyclic polyethers and their complexes with metal salts, *J. Am. Chem. Soc.* **89**: 7017-7036 (1967).
- Yordanov A.T., Roundhill D.M., *Solution extraction of transition and post-transition heavy and precious metals by chelate and macrocyclic ligands*, *Coord. Chem. Rev.* **170**: 93-124 (1998).
- Gloe K., Graubaus H., Wust M., Rambusch T., Seichter W., Macrocyclic and open-chain ligands with the redox switchable trithiadiazapentalene unit: synthesis, structures and complexation phenomena, *Coord. Chem. Rev.* **222**: 103-126 (2001).
- Buhlmann P., Pretsch E., Bakker E., Carrier based ion selective electrodes and bulk optodes. 2. Ionophores for potentiometric and optical sensors, *Chem. Rev.* **98**: 1593-1687 (1998).
- de Silva A.P., Gunaratne H.Q.N., Gunnlaugsson T., Huxley A.J.M., McCoy C.P., Rademacher J.T., Rice T.E., Signaling recognition events with fluorescent sensors and switches, *Chem. Rev.* **97**: 1515-1566 (1997).
- Masteri-Farahani M., Tayyebi N., A new magnetically recoverable nanocatalyst for epoxidation of olefins, *J. Mol. Catal. A: Chem.* **348**: 83-87(2011).
- Masteri-Farahani M., Kashef Z., Synthesis and characterization of new magnetically recoverable molybdenum nanocatalyst for epoxidation of olefins, *J. Magn. Magn. Mater.* **324**: 1431-1434 (2012).
- Mohammadikish M., Masteri-Farahani M., Mahdavi S., Immobilized molybdenum-thiosemicarbazide Schiff base complex on the surface of magnetite nanoparticles as a new nanocatalyst for the epoxidation of olefins, *J. Magn. Magn. Mater.* **354**: 317-323 (2014).
- Masteri-Farahani M., Bahmanyar M., Mohammadikish M., Organic-inorganic hybrid nanomaterials prepared from 4-formyl benzo-12-crown-4-ether and silica coated magnetite nanoparticles, *J. Nanostructures* **1**: 191-197 (2012).
- Rofouei M.K., Rezaei A., Masteri-Farahani M., Khani H., Selective extraction and preconcentration of ultra-trace level of mercury ions in water and fish samples using Fe₃O₄-magnetite-nanoparticles functionalized by triazene compound prior to its determination by inductively coupled plasma-optical emission spectrometry, *Anal. Methods* **4**: 959-966 (2012).
- Buchanan G.W., Driega A.B., Moghimi A., Bensimon C., Kirby R.A., Bouman T.D., Benzo-9-crown-3 ether: X-ray crystal structure, NMR studies in solution and the solid phase, and ab initio calculations of isotropic ¹³C chemical shifts using LORG with a D95V basis set, *Can. J. Chem.* **71**: 1983-1989 (1993).
- Cai Q., Lin W.Y., Xiao F.S., Pang W.Q., The preparation of highly ordered MCM-41 with extremely low surfactant

- concentration, *Micropor. Mesopor. Mater.* **32**: 1-15 (1999).
33. Sutra P., Fajula F., Brunel D., Lentz P., Daelen G., Nagy J.B., ^{29}Si and ^{13}C MAS-NMR characterization of surface modification of micelle-templated silicas during the grafting of organic moieties and end-capping, *Colloids and Surfaces A: Physicochem. Eng. Aspects* **158**: 21-27 (1999).
34. Lim M.H., Stein A., Comparative studies of grafting and direct syntheses of inorganic-organic hybrid mesoporous materials, *Chem. Mater.* **11**: 3285-3295 (1999).
35. Gregg S.J., Sing K.S.W., *Adsorption, Surface area and Porosity*, Academic Press, London, (1982).